Journal of Oleo Science
Copyright ©2012 by Japan Oil Chemists' Society
J. Oleo Sci. **61**, *(1) 1-9 (2012)*

Crystallization Kinetics of Organogels Prepared by Rice Bran Wax and Vegetable Oils

Lakmali Samuditha K. Dassanayake[1], Dharma R. Kodali[2, 3*], Satoru Ueno[1*] and Kiyotaka Sato[1]

[1] *Laboratory of Food Biophysics, Graduate School of Biosphere Science, Hiroshima University (Kagamiyama 1-4-4, 739-8528, JAPAN)*
[2] *Global Agritech, Inc. (710 Olive Ln., Minneapolis, MN 55447, UNITED STATES)*
[3] *Department of Bioproducts and Biosystems Engineering, University of Minnesota (1390 Eckles Avenue, St. Paul, MN 55108, UNITED STATES)*

Abstract: Rice bran wax (RBX) obtained during rice bran oil purification can form organogels in edible oils. The kinetics of crystallization and the viscous properties of RBX organogels were studied using differential scanning calorimetry (DSC), viscosity changes with varying temperature, hardness measurements by penetrometry, and synchrotron radiation X-ray diffraction (SR-XRD). The organogels were prepared by RBX in concentrations of 1%, 3%, 6%, and 10% on a weight basis in salad oil, olive oil, and camellia oil. The liquid oil type had no significant effect on the melting and crystallization temperatures of the RBX. However, the viscosity and the texture of the organogels differed with liquid oil type, temperature, and RBX concentration. Changes in the viscosity of the RBX organogels were monitored during cooling from 80°C to 20°C. Drastic viscosity changes occurred in accordance with the onset of crystallization in DSC thermographs obtained at a rate of 5°C/min. RBX in the olive oil and camellia oil mixtures had higher viscosity than RBX in the salad oil mixture, which correlates with the hardness obtained in texture measurements at 20°C. SR-XRD was used to clarify the crystal structures of the building blocks of the RBX organogels in salad oil. It was found that the RBX formed crystals with a long spacing of 7.3 ± 1 nm and short spacings of 0.41 ± 1 nm and 0.37 ± 1 nm. The intensity of the long-spacing pattern was remarkably weaker than that of the short-spacing patterns, which demonstrated strong anisotropy in the crystal growth of RBX crystal particles.

Key words: crystallization kinetics, organogels, rice bran wax, synchrotron radiation x-ray diffraction, viscosity

1 INTRODUCTION

Many sensory attributes of foods (e.g., spreadability, mouthfeel, snap, and texture) depend on the fat crystal network, which is comprised mainly of high-melting fats[1)]. Thus far, high-melting fats containing *trans* fatty acid and saturated fatty acid moieties have been employed. However, it has recently been claimed that the intake of high levels of *trans* and saturated fats contribute to global epidemics related to metabolic syndrome and cardiovascular disease[2)]. These negative health implications can be reversed by altering the intake and replacing unhealthy fats with healthier alternatives. To achieve this, novel technologies for structuring edible oils must be implemented[3-7)]. To address this challenge, organogels were introduced as alternative oil-structuring materials that have physical, chemical, and organoleptic properties similar to those of conventional high-melting fats; that are cost-effective and food-grade; and that have no negative health effects[3-19)]. Organogels are gels with a liquid phase comprised of oil[5)]. Gelators form continuous gel networks of small molecules that assemble into liquid crystals, micelles, or self-assembled fibrous networks[4, 8)].

In our previous publication[16)], we reported that rice (*Oryza sativa*) bran wax derived from rice bran, as a by-product of rice milling, can be used as a good organogelator to fulfill most of the requirements expected in food applications. We found that a mixture of RBX and olive oil at a concentration ratio of 1:99 wt% formed organogel at 20℃, whereas the lowest concentration necessary for Carnauba wax (CRX) to form organogel in olive oil was 4wt% and that for Candellila wax (CLX) was 2 wt%. The RBX crystals melted in the bulk state at 77℃ to 79℃ with $\Delta H_{melting}$ = 190.5 J/g, which is quite high compared with CLX (129 J/g) and CRX (137.6 J/g). The XRD data for the RBX crystals

*Correspondence to: S. Ueno, Laboratory of Food Biophysics, Graduate School of Biosphere Science, Hiroshima University, Kagamiyama 739-8528, JAPAN; D. R. Kodali, Global Agritech, Inc., 710, Olive Ln. Minneapolis, MN 55447, US.
E-mail: sueno@hiroshima-u.ac.jp; kodali@globalagritech.us
Accepted August 18, 2011 (received for review June 10, 2011)
Journal of Oleo Science ISSN 1345-8957 print / ISSN 1347-3352 online
http://www.jstage.jst.go.jp/browse/jos/ http://mc.manusriptcentral.com/jjocs

revealed $O_{\perp}$ subcell packing and a long spacing of 6.9 nm. Tiny needle-shaped crystals were observed in the mixtures of RBX and liquid oils (olive oil and salad oil). These results demonstrate a high possibility of organogel-forming properties in RBX, mostly because it forms long, needle-like crystals finely dispersed in liquid oil phases.

The principles behind organogel formation, crystal network formation, and their functionality are the most important areas to be studied, as they are unique to the organogelators used as well as playing crucial roles in the structure of the product. The identification and quantification of the structural organization of food systems provide insight into the relationships among the composition, processing, structure, and mechanical properties of the networks formed. However, comprehensive knowledge of structural network characteristics is still lacking[1], and organogels have been underutilized thus far, due to the inability to modify or predict the microstructure of the fibrous network structure[20].

From the perspective of structuring liquid oil using RBX, continued in-depth studies of the physico-chemical properties of organogels at the micro level are of utmost importance. The best approach to obtaining detailed knowledge of these properties is to start from the molecular arrangement adopted by the components of the system[21, 22]. Fundamental research on the molecular characteristics of RBX organogels would help in the modification of the macroscopic properties of the gels.

In our first paper[16], we reported the formation of organogel in mixtures of RBX and vegetable oils in comparison to the organogels formed in mixtures of carnauba wax and candelilla wax. This work was the first to show that RBX can be a good organogelator. However, the kinetic properties of organogel formation, which are determined in detail by the rate of crystallization of rice bran wax, were not examined in this work. The most advantageous property of RBX-based organogel compared to the other plant wax-based organogels is its rate of organogel formation, which is governed by the rate of crystallization. We therefore presented the kinetic properties of organogel formation of RBX using XRD, DSC, and viscosity measurements.

The purpose of using different vegetable oils in this study was to evaluate the effect of liquid oil type on gelation and other physical characteristics of RBX-vegetable oil mixtures. Olive oil and salad oil are commonly used in food as edible oils, whereas camellia oil is used mostly for cosmetics rather than for edible purposes. Terech et al. reported that the nature of the solvent can also influence gelation[23]. Burkhardt et al. studied the correlation between the polarity of the solvent and the amount of gelator required for gelation in organogels prepared using 12-hydroxystearic acid (HSA). The required amount of HSA for gelation increased with more polar solvents. The appearance of formed organogels differs with HSA concentration and solvent type[24]. However, the appearance of RBX-vegetable oil organogels differs only with RBX concentration and not with solvent type.

2 EXPERIMENTAL PROCEDURES

2.1 Materials and sample preparation

RBX was supplied by Global Agritech, Inc., Minneapolis, MN USA. RBX was blended with salad oil (canola: soybean oil = 50:50) [C16:0 8.3%, C18:1 38.1%, C18:2 40.3%, C18:3 7.9%] (Nisshin OilliO, Japan), olive oil (J-Oil Mills, Japan), and camellia oil (Yokozeki Oil and Fat Industries Co., Japan) at 1, 3, 6, and 10 wt% levels. Samples were prepared by dissolving the weighed solid waxes in a weighed amount of liquid oil at 80℃, which was sufficient to obtain full melting of all components. The heated solutions were subsequently cooled to room temperature (20℃) and stored at this temperature. All concentrations discussed here are expressed as a weight percentage (wt%).

2.2 Thermal analysis

The melting temperature (T_m) and crystallization temperature (T_c) of RBX-vegetable oil organogels were determined by differential scanning calorimetry (DSC) using a Rigaku DSC-8240 calorimeter (Rigaku, Tokyo, Japan). Samples (10 to 15 mg) were hermetically sealed in aluminum pans, heated from room temperature to 100℃, then cooled to 0℃, and heated again to 100℃. The rate of temperature variation was 5℃/min for heating and cooling. The peak T_m, T_c, melting enthalpy (ΔH_m), and crystallization (ΔH_c) were determined using the software provided with the instrument. DSC measurements were carried out in triplicate for RBX in liquid oils. The average endothermic peak value was taken as T_m.

2.3 Crystal morphology

The RBX crystals formed in olive oil were observed with polarized optical microscopy. The crystal morphology was compared at different solute concentrations of RBX at 1 wt%, 6 wt%, and 10 wt%. The mixtures of RBX and olive oil were prepared by adding an appropriate amount of waxes to the liquid oils and heating to 80℃ to form a homogenous solution. The solutions were cooled to room temperature until wax crystals formed. The crystals were observed by polarized light microscopy using an Olympus CX31 PF Optical microscope (Olympus Optical Co., Ltd., Japan). A small amount of sample containing crystals was placed on a glass microscope slide and gently covered with a glass cover slip. Digital images of partially and fully polarized specimens were acquired using an Olympus DP12-2 camera (Olympus Corporation, Japan).

2.4 Viscosity measurements

The viscosity of the RBX-vegetable oil organogels was measured during cooling using a Vibro Viscometer SV-10 (A & D, Japan) with a Thermo-mate BF 400 (Yamato, Japan). This viscometer uses a frequency of 30Hz at constant frequency and amplitude. The effect the of type of vegetable oil on the viscosity of the organogels was measured for all concentrations of RBX in salad oil, olive oil, and camellia oil.

The prepared gel samples were heated to 80℃ for complete melting. The melted sample was placed in the sample cell of the viscometer at 80℃, and two gold-plated paddle sensors were immersed in the sample. The viscosity change of the sample was then measured with respect to the temperature during cooling from 80℃ to 20℃ at a rate of ~ 1℃/min. The measured viscosity for each sample was plotted against the temperature.

2.5 Hardness measurements

An EX-120-E Penetrometer (Elex Scientific, Tokyo, Japan) was used to measure the hardness of the organogels made of RBX in vegetable oils. The sample cups in which the samples were kept during the measurement had an internal diameter of 5.5 cm and a depth of 3.4 cm. Each sample cup included a glass container filled with water to maintain a constant temperature during the measurement. The internal diameter of the glass container was 10.7 cm, and its depth was 6 cm. The conical plastic probe of the penetrometer had a base diameter of 16.25 ± 0.015 mm, a cone height of 7.075 ± 0.015 mm, and a weight of 9.38 ± 0.025 g. A load weighing 50 g was placed on the sample in each penetration. The penetration depth was measured three times for each sample at 20℃, and average values were calculated.

2.6 Synchrotron radiation X-ray diffraction analysis

Synchrotron radiation X-ray diffraction (SR-XRD, λ = 0.15 nm) studies were conducted at the Photon Factory (PF, BL-15A) at the National Laboratory for High-Energy Physics, Tsukuba, Japan. The PF operates at 2.5 GeV. XRD spectra were recorded every 30 seconds using two gas-filled one-dimensional position-sensitive detectors. One detector was for the small-angle region (Rigaku, Tokyo, 512 channels over a total length of 200mm); the other was for the wide-angle region (MAC Science, Tokyo, 512 channels over a total length of 50mm). The distances between the sample and detector were 1280 mm (small-angle) and 280 mm (wide-angle). The temperature of the sample was controlled by two water baths and recorded in combination with XRD data collection. The 2% RBX-salad oil organogel was heated to melt and XRD spectra were recorded during cooling from 80℃ to 20℃.

3 RESULTS AND DISCUSSION

Cooling and heating thermograms for RBX in salad oil, olive oil, and camellia oil mixtures at a concentration of 1% (wt) are presented in Fig. 1. The thermal behavior of the RBX-vegetable oil mixtures was examined during cooling to 0℃ after melting at 100℃, and during re-heating of the first crystallized material from 0℃ to 100℃. The cooling and heating rates were 5℃/min. Regardless of the type of vegetable oil used, RBX exhibited broad DSC melting peaks with an indefinite start and a blunt maximum, as we observed in earlier investigations of bulk RBX and RBX-salad oil, olive oil, and liquid paraffin mixtures in different RBX concentrations at a rate of 2℃/min for cooling and heating[16].

RBX is a natural product with a complex composition created by esterified long-chain fatty acids and long-chain fatty alcohols of different chain lengths, along with various other minor components, which explains the presence of broad exothermal and endothermal peaks[16]. RBX exhibited clear single exotherms in all of the oil mixtures, indicating that all of the components in RBX form crystals over a considerably narrow temperature range (3.3 ± 0.2℃). The onset of crystallization, peak top, and the end set of crystallization temperatures are indicated in the figure. RBX-olive oil and RBX-camellia oil mixtures have more similar melting and crystallization temperatures than RBX-salad oil mixtures.

During heating, RBX-vegetable oil mixtures exhibited much broad (24.6 ± 0.8℃) endotherms, with one prominent peak and two shoulder peaks on either side of the endothermic peak. This behavior is quite different from what we observed previously with bulk RBX and higher concentrations (>1%wt) of RBX in salad oil at a heating rate of 2℃/min[16]. Figure 1 presents the onset of melting, three peak top temperatures, and the end set of melting temperatures. CLX, a natural plant wax that has organogel-formation ability, exhibited similar thermal behavior during cooling and heating of CLX-safflower oil mixtures[14, 15] and in its bulk state[16]. Earlier authors explained this occurrence of multiple crystallization and melting profiles of CLX as due to the development of mixed molecular packing of *n*-alkanes present in CLX[14, 15]. However, the long-chain fatty acids and fatty alcohol esters present in RBX do not tend to form such mixed self-assembled structures with a lower extent of three-dimensional molecular structure[16]. These multiple peaks in the melting profile of RBX tend not to be visible at higher RBX concentrations (>1%wt.). Thus, melting of the less dominant fatty acid and fatty alcohol esters becomes less prominent, due to the melting of more abundant fatty acid and fatty alcohol esters in the higher levels of RBX-vegetable oil mixtures. Almost all of the combinations of RBX-vegetable oil mixtures in Fig. 1 exhibit similar thermal behavior, although RBX-salad oil mixtures have values that deviate from the rest. This result

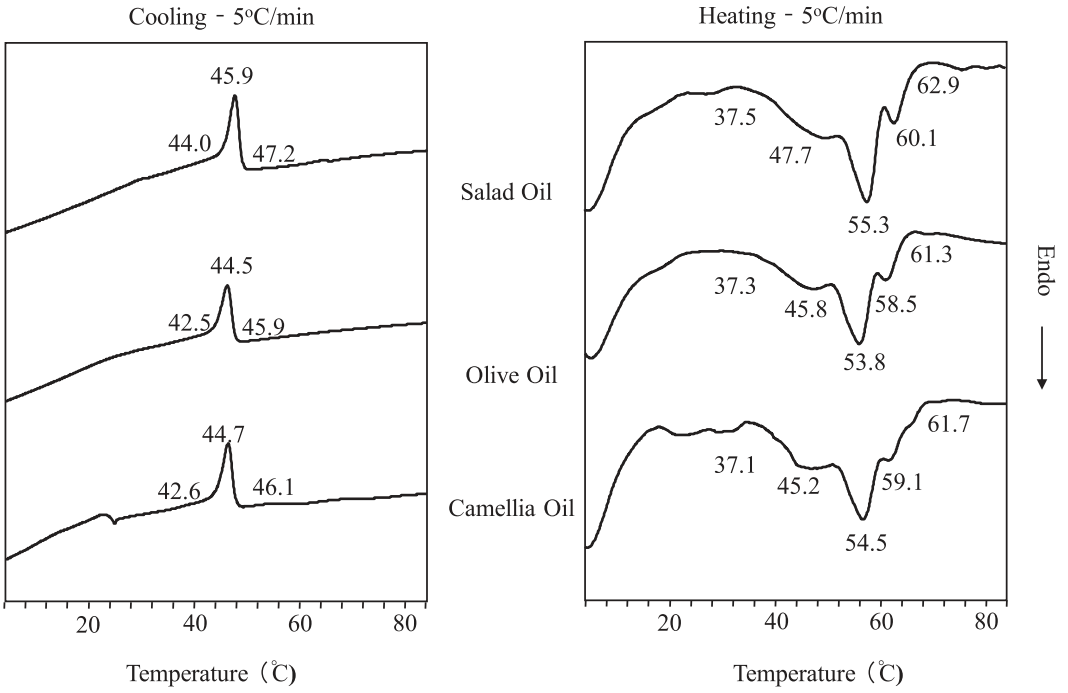

Fig. 1 DSC Measurements of mixtures of RBX in different oils [1 % (w/w)].

indicates that the liquid component does not affect the thermal properties of the organogel, which is solely governed by the solid component or the organogelator that causes the network to entrap the liquid oil to produce the organogel.

Figure 2 presents optical micrographs of crystals of RBX in olive oil taken at room temperature. We compared the crystal morphologies of different RBX concentrations in olive oil. The RBX crystals had a very long needle shape, which is a desirable feature for gel formation[23, 25]. The size of the crystal increased proportionately with increased RBX concentration. RBX crystals at 10% (w/w) in an olive oil mixture exhibited thick crystals 100 μm or longer, whereas crystals at 1% (w/w) in olive oil were 20 to 50 μm long. The long needle-like structures of RBX form a good crystal matrix that meshes well at the crystal-crystal interfaces to form organogels; this crystal morphology enables the entrapment of large volumes of liquid oils in crystalline scaffolding[16]. Therefore, we can expect that the interaction between RBX crystals and gel strength may improve in proportion to the solute concentration. Regarding the effects of liquid oils on the crystal morphology of RBX, no difference was observed in crystal morphology between olive oil and salad oil (data not shown).

Organogel hardness is a critical factor in industrial applications. Neither harder nor softer states are considered a favorable quality for organogels. The hardnesses of RBX-vegetable oil mixtures measured at 20℃ are presented in Fig. 3. Since the 1%wt level was much softer, no penetration experiments were conducted for those samples. The depth (mm) to which the penetration probe of the instrument penetrated in the gel was used to evaluate hardness, with larger values of penetration depth indicating a softer gel structure. In previous investigations, RBX had comparatively greater hardness than other plant waxes in olive oil[16]. At 3% and 6% (w/w) levels, RBX in olive oil formed softer gels than in the other two vegetable oils, and at 10% (w/w), RBX in olive oil formed the hardest gel among all of the tested samples. RBX formed softer gels with salad oil at all the tested concentrations, and no difference in hardness was observed for 6% and 10% (w/w) RBX in salad oil gels. At 3% (w/w), RBX formed the hardest gel with camellia oil; at 6% and 10% (w/w), RBX in the same oil exhibited medium hardness compared to that in the other two vegetable oils.

Figure 4 presents the changes in viscosity with temperature of organogels prepared with 1% (w/w) RBX in the three vegetable oils. The viscosity of the organogels was measured during cooling from 80℃ to 20℃. RBX-olive oil had the highest viscosity, and RBX-salad oil organogels had the lowest viscosity during the cooling process. RBX-olive oil organogel had nearly three times higher viscosity than the maximum viscosity of RBX-salad oil organogel. Furthermore, no significant difference was observed between the maximum viscosities presented by the olive oil and camellia oil with RBX at the end of cooling. In a previous investigation, we demonstrated that gel viscosity changes occurred at the same temperature as the onset of crystallization[16]. This is also clear when considering the exotherms of the three organogels presented in Fig. 1.

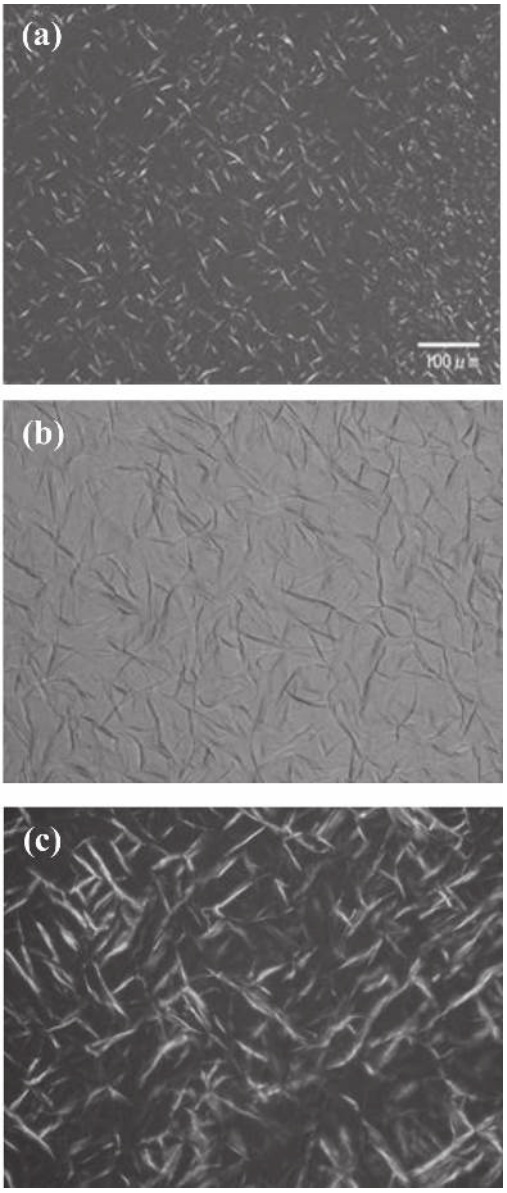

Fig. 2 Optical micrographs of RBX crystals (a) 1 %, (b) 6 %, (c) 10 % w/w in olive oil.

Similar viscosity changes were observed during heating (data not shown). All three samples reached minimum viscosities at temperatures equal to the end set temperatures of the DSC endotherms.

As for the effects of liquid oil type, the RBX-salad oil mixture displayed rather deviated characteristics in gelation (Fig. 1), gel strength (Fig. 3), and viscous properties (Fig. 4), compared to the RBX-olive oil and RBX-camellia oil mixtures. The major fatty acid composition of olive oil is Oleic (18:1) −78.0%, Linoleic (18:2) −8.3%, Linolenic (18:3) −0.8%, Palmitic (16:0) −8.4%, Stearic (18:0) −2.5%[26]. Camellia oil possesses similar fatty acid composition: Oleic (18:1) −82.0%, Linoleic (18:2) −6.8%, Linolenic (18:3) −0.4%, Palmitic (16:0) −7.9%, Stearic (18:0) −

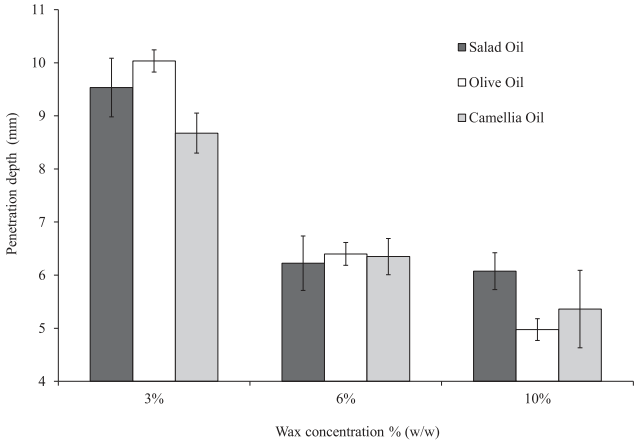

Fig. 3 Hardness measurements of the mixtures of RBX and 3 oils examined by penetrometry at 20°C.

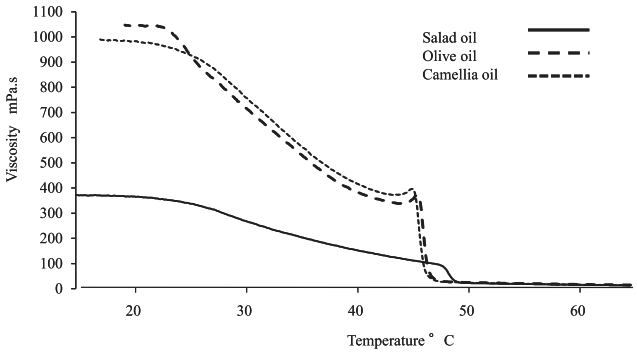

Fig. 4 Changes in viscosity during cooling process of RBX [1 % (w/w)] in three liquid oils.

1.8%, Eicosaenoic (20:1) −0.6%[27]. The salad oil used in this study was a blend of canola oil containing Oleic (18:1) −61.6%, Linoleic (18:2) −21.7%, Linolenic (18:3) −9.6%, Palmitic (16:0) −3.6%, Stearic (18:0) −1.5%, Eicosaenoic (20:1) −1.4%[26], and soybean oil containing Oleic (18:1) −23.8%, Linoleic (18:2) −53.3%, Linolenic (18:3) −7.6%, Palmitic (16:0) −10.8%, Stearic (18:0) −4.0%[26]. The viscosity of salad oil is lower than that of the other two oils (Fig. 4), and the hardness of the 10% concentration is lower for salad oil than for the other two (Fig. 3). The liquid oil type should therefore have some effect, since organogels using salad oil are softer than those using olive oil and camellia oil. This result may be due to the increased concentration of oleic acid and the decreased concentration of linoleic acid for olive oil and camellia oil, compared with salad oil. Therefore, RBX crystals are more soluble in salad oil than in the other two oils, and the strength of the crystal network of RBX in salad oil organogel may be reduced at the crystal junctions.

A large increase in the maximum viscosity of RBX-salad oil gels in the cooling process was observed with increasing RBX concentrations (Figs. 5 and 6). At 3% (w/w) RBX, the maximum viscosity achieved is more than three times

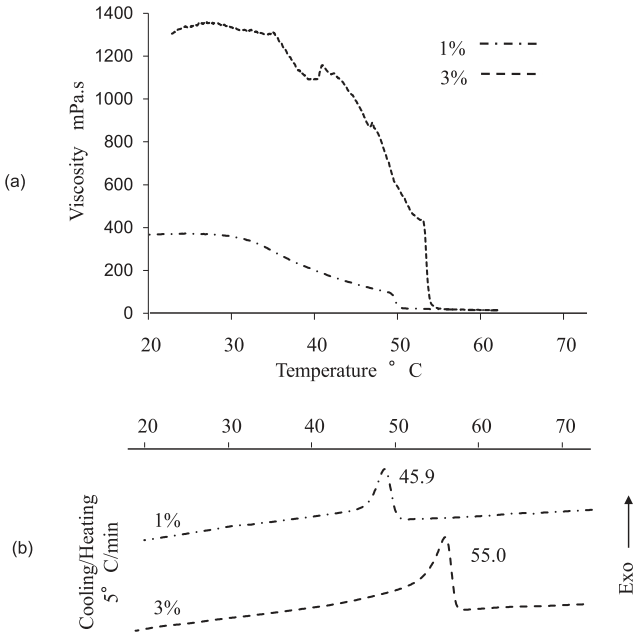

Fig. 5 (a) Changes in viscosity during cooling process and (b) DSC cooling thermograms of RBX [1 % and 3 % (w/w)] in salad oil mixtures.

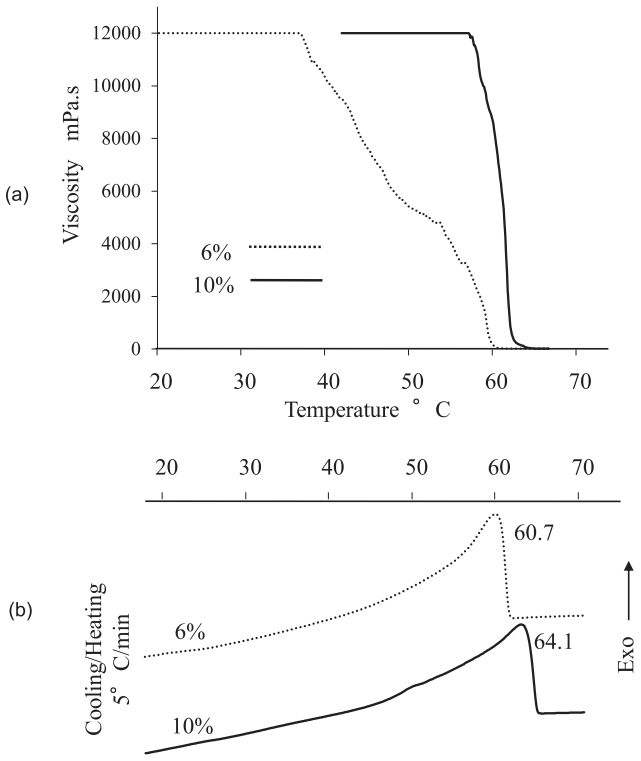

Fig. 6 (a) Changes in viscosity during cooling process and (b) DSC cooling thermograms of RBX [6 % and 10 % (w/w)] in salad oil mixtures.

higher than at 1% (w/w) RBX. The maximum viscosity of the same mixture is 10 times higher than at 3% (w/w) with RBX concentrations of 6% (w/w) and 10% (w/w) (Figs. 5a and 6a). Interestingly, at 10% (w/w), once the RBX-salad oil mixture reached the onset of crystallization temperature the viscosity level increased linearly to its maximum value over a short range of temperature decline, while at 6% (w/w) it required a much broader range of temperature difference (20℃) to reach maximum viscosity. Changes in the viscosity of RBX-vegetable oil gels occurred in parallel with changes in the thermal properties displayed by the DSC exotherms (Figs. 5b and 6b). This is always applicable regardless of the RBX concentration and the type of liquid oil used.

The effect of wax concentration on hardness and viscosity is also explained by crystal behavior, size, shape and thermal kinetics. Fiber-like needle crystals form a strong gel network, leading to high melting and crystallization points[16]. As depicted in Fig. 2, higher RBX levels form comparatively longer and thicker fibrous crystals, which help to create a strong crystal network; thus, highly viscous and hard organogels form.

Figure 7 depicts small and wide-angle SR-XRD patterns that were simultaneously measured with DSC, taken during the cooling process of 2% (w/w) RBX-salad oil gels. Lakmali Samuditha K. Dassanayake[1], Dharma R. Kodali[2, 3]*, S. Ueno[1]* and K. Sato (b) depicts a DSC cooling thermogram for a sample that was initially heated to 100℃ and then cooled to 0℃ at a rate of 5℃/min. The onset of the endothermic peak was 52℃, and the peak top temperature was 51℃.

The powerful X-ray beam obtained from the synchrotron source enables a complete and detailed X-ray diffraction spectra compared to powder XRD studies, especially in the small-angle region. The short-spacing spectra agree with the powder XRD studies of bulk RBX and 8% (w/w) RBX-olive oil gels observed earlier[16]. However, the long-spacing spectra obtained from SR-XRD do not agree with the powder XRD observations[16]. Considering the reliability of SR-XRD and its potential to improve on powder XRD in producing diffraction spectra in small-angle regions, the d-spacings obtained by SR-XRD could become the accepted values.

Figure 7a depicts small and wide-angle SR-XRD spectra taken at 30-second intervals with a 10-second exposure time. Soon after 52℃ was reached, a small peak with a long spacing of 7.4 nm appeared in the small-angle region. Upon cooling, the peak remained constant up to 0℃. Correspondingly, short-spacing spectra of 0.41 nm and 0.38 nm appeared at 52℃ in the wide-angle region. This result indicates the orthorhombic perpendicular ($O_{\perp}$) subcell packing that was characterized in RBX in previous investigations[16, 25]. Similar structures are found for most natural plant waxes and beeswax[28-31]. The remarkably weaker intensity of long-spacing patterns compared with that of short-spacing patterns demonstrates strong anisotropy in crystal growth

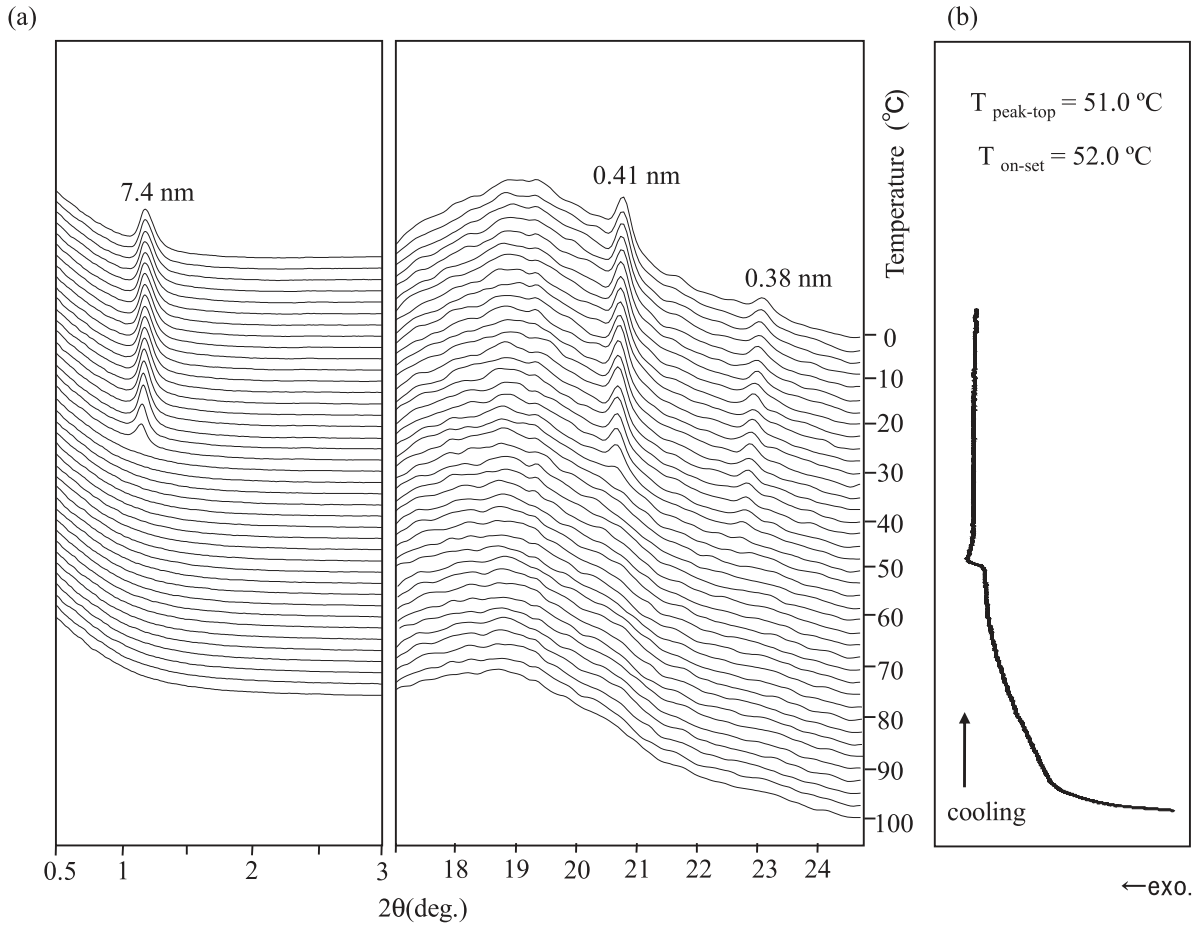

Fig. 7 Synchrotron radiation X-ray diffraction spectra (a) and DSC cooling thermogram (b) of Rice bran wax (2 % w/w) in salad oil.

rates between directions vertical to the lamellar plane and within the lamellar plane. This result has been verified and is in agreement with powder XRD analysis[16, 25]. Kodali[25] stated that the molecular interactions within the lamellar planes are far greater than those through the end methyl groups due to van der Waals interaction between the long hydrocarbon chains and polar ester functional groups. This property leads to a faster crystal growth rate within the lateral plane and an extremely slow crystal growth rate through the end methyl plane. This unique crystal growth of RBX leads to either needle or platelet crystal morphology, as observed in Fig. 2. Recent cryo-TEM (transmission electron microscopic) analysis of fat crystals in liquid oil revealed such crystal morphologies as thin plate and long needle plate of nanometer scale dimensions[32, 33].

Figure 8 plots the temperature dependence of the intensity of the small-angle XRD peaks (7.4 nm in Fig. 7a) of RBX in salad oil, which were taken using SR-XRD during cooling from 100℃ to 0℃. The intensity of each peak was calculated from the total area of the diffraction spectrum at each temperature. The spectral intensity began to increase at 49℃ and increased rapidly around 40℃, reaching

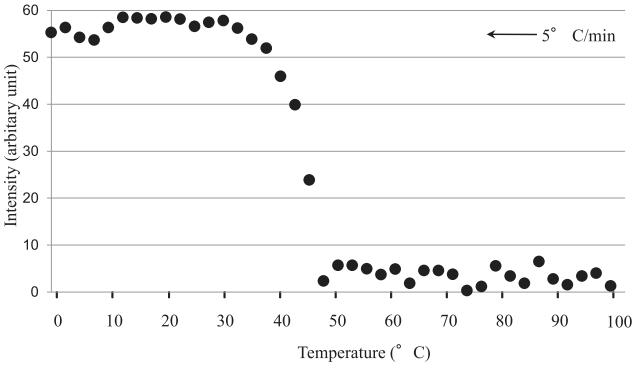

Fig. 8 Temperature dependence of the intensity of SAXS diffraction peaks (7.4 nm in Fig. 7a) of 2 % (w/w) rice bran wax in salad oil.

a plateau at 30℃. This feature of the XRD peak intensity variation with temperature also corresponds well with the DSC cooling exothermic peak in Fig. 7b. However, Fig. 8 more clearly indicates that the rate of crystallization of RBX is quite high and that the network of the RBX crystals was formed rapidly, as indicated by viscosity measure-

ments (Figs. 4-6).

4 CONCLUSION

The crystallization kinetics of organogels prepared using RBX and different liquid oils were studied to find candidates for structured oils, namely organogels, without TAGs. The high thermal stability, crystallinity, and strength of the RBX organogels were emphasized by the high melting temperatures and crystal morphology of the thin, needle-shaped crystals of RBX, which caused a sharp increase in viscosity during the cooling process. The crystallization kinetics of organogels was somewhat affected by the type of liquid oil used: salad oil had softer organogels than olive oil and camellia oil. The reasons for the differences in organogels using the three vegetable oils are associated with differences in the TAG composition of the vegetable oils, which in turn result in different viscosities of the RBX crystal dispersion and different hardnesses of the RBX organogels. The vegetable oils containing TAGs consist of saturated fatty acids and high melting fatty acids cause highly viscous and hard organogels. In particular, the organogels of RBX with olive oil and camellia oil were much harder than that with salad oil, because the former oils included high-melting fatty acids, namely oleic and palmitic acids, which increased the viscosity of the organogels and the rate of crystallization of the RBX.

However, the RBX concentration exhibited the most significant effect on organogel characteristics, as demonstrated by microscopy and by viscosity and hardness evaluations. SR-XRD results provided evidence of tight packing of RBX crystals in an orthorhombic perpendicular ($O_{\perp}$) subcell structure.

ACKNOWLEDGEMENTS

This experiment has been performed under the approval of the Photon Factory Program Advisory Committee (Proposal No. 2008G201 and 2010G114). The authors highly appreciate associate professor N. Igarashi, the station manager of BL-15A, Photon Factory, KEK Institute, Tsukuba, Japan.

References

1) Narine S. S.; Marangoni A. G. *Microstructure in Fat Crystal Networks* (Marangoni, A. G. ed.) Marcel Dekker. New York. pp 179-180 (2005).
2) Schrimpf-Moss J.; Wilkening V. Trans Fat-New FDA Regulations. in *Trans Fats Alternatives*. (Kodali, D. R.; List G. R. ed.) AOCS Press. Champaign, Illinois. pp. 26-28 (2005).
3) Rogers M. A.; Wright A. J.; Marangoni A. G. Crystalline stability of self-assembled fibrillar networks of 12-hydroxystearic acid in edible oils. *Food Res. Int.* **41**, 1026-1034 (2008).
4) Rogers M. A.; Wright A. J.; Marangoni A. G. Nanostructuring fiber morphology and solvent inclusions in 12-hydroxystearic acid/canola oil organogels. *Curr. Opinion in Coll. & Inter. Sci.* **14**, 33-42 (2009).
5) Rogers M. A. Novel structuring strategies for unsaturated fats-Meeting the zero-trans, zero-saturated fat challenge: A review. *Food Res. Int.* **42**, 747-753 (2009).
6) Hughes N. E.; Marangoni A. G.; Wright A. J.; Rogers M. A.; Rush J. W. E. Potential food applications of edible oil organogels. *Trends in Food Sci. & Tech.* **20**, 470-480 (2009).
7) Pernetti M.; van Malssen K. F.; Flöter E.; Bot A. Structuring of edible oils by alternatives to crystalline fat. *Curr. Opinion in Coll. & Inter. Sci.* **12**, 221-231 (2007).
8) Abdallah D. J.; Weiss R. G. Organogels and Low Molecular Mass Organic Gelators. Adv. *Mater.* **12**, 1237-1247 (2000).
9) Bot A.; Agterof W. G. M. Structuring of edible oils by mixtures of γ-oryzanol with β-sitosterol or related phytosterols. *J. Am. Oil Chem. Soc.* **83**, 513-521 (2006).
10) Bot A.; Veldhuizen Y. S. J.; den Adel R.; Roijers E. C. Non-TAG structuring of edible oils and emulsions. *Food Hydrocoll.* **23**, 1184-1189 (2009).
11) Wright A. J.; Marangoni A. G. Formation, structure, and rheological properties of ricinoelaidic acid-vegetable oil organogels. *J. Am. Oil Chem. Soc.* **83**, 497-503 (2006).
12) Wright A. J.; Marangoni A. G. Time, temperature, and concentration dependance of ricinoelaidic acid-canola oil organogelation. *J. Am. Oil Chem. Soc.* **84**, 3-9 (2007).
13) Pernetti M.; van Malssen K.; Kalnin D.; Flöter E. Structuring edible oil with lecithin and sorbitan tri-stearate. *Food Hydrocoll.* **21**, 855-861 (2007).
14) Toro-vazquez J. F.; Morales-Rueda J. A.; Dibildox-Alvarado E.; Charó-Alonso M.; Alonzo-Macias M.; González-Chávez M. M. Thermal and textural properties of organogels developed by candelilla wax in safflower oil. *J. Am. Oil Chem. Soc.* **84**, 989-1000 (2007).
15) Morales-Rueda J. A.; Dibildox-Alvarado E.; Charó-Alonso M. A.; Weiss R. G.; Toro-Vazquez J. F. Thermomechanical properties of candelilla wax and dotriacontane organogels in safflower oil. *Eur. J. Lipid Technol.* **111**, 207-215 (2009).
16) Dassanayake L. S. K.; Kodali D. R.; Ueno S.; Sato K. Physical properties of rice bran wax in bulk and organogels. *J. Am. Oil Chem. Soc.* **86**, 1163-1173

(2009).
17) Higaki K.; Sasakura Y.; Koyano T.; Hachiya I.; Sato K. Physical analysis of gel-like behavior of binary mixtures of high- and low-melting fats. *J. Am. Oil Chem. Soc.* **80**, 263-270(2003).
18) Higaki K.; Sasakura Y.; Koyano T.; Hachiya I.; Sato K. In situ optical observation of microstructure of β-fat gel made of binary mixtures of high-melting and low-melting fats. *Food Res. Int.* **37**, 2-10(2004 a).
19) Higaki K.; Sasakura Y.; Koyano T.; Hachiya I.; Sato K. Rheological properties of β-fat gel made of binary mixtures of high-melting and low-melting fats. *Food Res. Int.* **37**, 799-804(2004 b).
20) Wang R.; Lui X-Y.; Xiong J.; Li J. Real-time observation of fiber network formation in molecular organogel: supersaturation dependent microstructure and its related rheological property. *J. Phys. Chem. B.* **110**, 7275-7280(2006).
21) Larsson K.; Quinn P.; Sato K.; Tiberg F. *Basic concepts in Lipids: Physical properties and functionality* (Larsson K.; Quinn P.; Sato K.; Tiberg F. ed.)The Oily Press. England. p. 6(2006).
22) Flöter E. The role of physical properties data in product development. *Eur. J. Lipid Sci. Tech.* **111**, 219-226(2009).
23) Terech P.; Weiss R. G. Low molecular mass gelators of organic liquids and the properties of their gels. *Chem. Rev.* **97**, 3133-3159(1997).
24) Burkhardt M.; Kinzel S.; Gradzielski M. Macroscopic poperties and microstructure of HSA based organogels: Sensitivity to polar additives. *J. Colloid Interface Sci.* **331**, 514-521(2009).
25) Kodali D. R. The utilization of rice bran wax to stabilize long chain ω-3 polyunsaturated fatty acid esters. *Lipid Tech.* **21**, 254-256(2009).
26) Firestone D. Olive Oil. in *Bailey's Industrial Oil & Fat Products*(Shahidi F. ed.)6th ed. Vol. 2, John Wiley & Sons Inc. New Jersey. p. 317(2005).
27) Haiyan Z.; Bedgood Jr. D. R.; Bishop A. G.; Prenzler P. D.; Robards K. Endogenous biophenol, fatty acid and volatile profiles of selected oils. *Food Chem.* **100**, 1544-1551(2007).
28) Kameda T. C-13 solid-state NMR analysis of heterogeneous structure of beeswax in native state. *J. Phys. D Appl. Phys.* **38**, 4313-4320(2005).
29) Ritter B.; Schulte J.; Schulte E. Detection of coating waxes on apples by differential scanning calorimetry. *Eur. Food Res. Technol.* **212**, 603 − 607(2001).
30) Ensikat H. J.; Boese M.; Mader W.; Barthlott W.; Koch K. Crystallinity of plant epicuticular waxes: electron and X-ray diffraction studies. *Chem. Phys. Lipids.* **144**, 45-59(2006).
31) Mellema, M. Co-crystals of beeswax and various vegetable waxes with sterols studied by X-ray diffraction and differential scanning calorimetry. *J. Am. Oil Chem. Soc.* **86**, 499-505(2009).
32) Acevedo, N. C.; Marangoni, A. G. Characterization of the nanoscale triacylglycerol crystal networks. *Cryst. Growth Des.* **10**, 3327-3333(2010).
33) Acevedo N. C.; Marangoni A. G. Toward nanoscale engineering of triacylglycerol crystal networks. *Cryst. Growth Des.* **10**, 3334 -3339(2010).